Trans. Of the Society of Instrument
and Control Engineers
Vol.E-1, No.1, 1/7 (2001)

Fast-scan Magnetic Resonance Imaging

Hideto Iwaoka, Hiroyuki Matsuura, Tadashi Sugiyama, and Takaaki Hirata

This paper describes the fast recovery (FR) method for fast-scan magnetic resonance imaging. The FR method uses a sequence of four radio frequency pulses: alternating selective 90° nutation pulses and nonselective 180° pulses. One free induction decay (FID) signal and one echo signal are detected and averaged to compute a 2-D image. In the modified FR method, extra 180° pulses are applied between 90° pulses to cause refocusing and the resultant spin echo signals are averaged to improve the signal-to-noise ratio. For the FR and modified FR sequences, the macroscopic magnetization is restored to equilibrium quickly and exactly; scan time can consequently be less than that for conventional pulse sequences, such as used in the saturation recovery method, without any penalty in signal-to-noise ratio.

This paper derives expressions for signal-to-noise ratio, scan time ratio and contrast noise ratio, compares the FR and modified FR methods with the saturation recovery method, and presents experimental results for human body images.

In theory and practice, the signal-to-noise ratio for the FR method is larger than that for the modified FR method. For a given signal-to-noise ratio, the scan time is between one half and one fourth that for the saturation recovery method. The optimum repetition period, T_r, is 0.07 - 0.25s for the FR method, and 0.1 - 0.5s for the modified FR method. The contrast noise ratio is low for high speed imaging, T_r = 0.07 - 0.25s, but a high contrast noise ratio image is obtained for T_r > 0.5s.

Key Words: magnetic resonance imaging, MRI, fast scan, scan sequence, S/N, CNR

1. Introduction

Magnetic resonance imaging (MRI) as a method to obtain cross-section images of the human body without injury using proton (^{1}H) nuclear magnetic resonance signals was proposed by Lauterbur [1]. The method attracted interest as a useful and new diagnosis, and practical equipment was developed. MRI presents no radiation hazard but the images have to be reconstructed from very low energy signals and low signal-to-noise ratio (S/N) and requires a long scan time due to the interval time in scan sequences during which there is no signal. Compared with X-ray computed tomography systems which have a scan time of 3 - 10 s, conventional MRI systems require a scan time of 60 - 300 s. If the scan time of MRI could be reduced, it would bring benefits of reduced diagnostic cost, physical and mental damage to patients, and motion artifacts. The image quality of MRI systems has recently been improved on a practical level, and further efforts to reduce the scan time and to be able to measure multi functions have been started [2),3)].

There are two well-known concepts for reducing the scan time, the first is to improve the hardware such as by adopting a strong magnet of up to 1.5 - 2T [4)], and the second is to improve the pulse sequence which means improving the algorithm that controls the behavior of the macroscopic magnetization M of proton (^{1}H). The first approach reduces the scan time without data averaging while improving S/N, as S/N is proportional to magnetic field strength. There have been several reports on the second approach such as:

1) Echo Planar method (EP) [5)]
2) Carr-Purcell-Meiboom-Gill method (CPMG) [6)]
3) Multi Slice method (MS) [7)]
4) Steady State Free Precession method (SSFP) [8)]
5) Fast Recovery method (FR) [9)].

EP can acquire an image in several tens of milliseconds, but S/N is not improved and the quality of the image is poor. CPMG can acquire many projection data signals of multi sections with one excitation pulse, but image characterization is very complex due to the spin-spin relaxation time (T_2). MS can obtain many projection data signals by exciting the slices one by one in the waiting time during which the macroscopic magnetization of a slice reaches thermal equilibrium, and the total scan time for a slice is not reduced. SSFP can successfully obtain all data signals without waiting for M to reach thermal equilibrium, but the image contrast is not sufficient. The authors have already proposed a new pulse sequence named Fast Recovery method (FR) for fast scans and reported the analysis and experimental results using small magnet equipment[9)-11)]. This paper reports the fast scan capability and high quality image of FR by analyzing S/N, scan time, image contrast between tissues, and the experimental results of imaging of the human head.

Yokogawa Electric Corporation
2-9-32, Naka-cho, Musashino-shi, Tokyo 180-8750, Japan
Phone: +81-422-55-5753 Fax: +81-422-55-7044
e-mail : hideto.iwaoka@jp.yokogawa.com

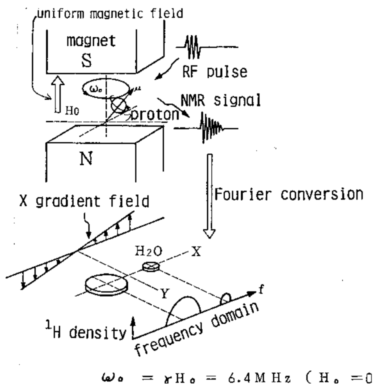

(a) Resonance, detection and image reconstruction

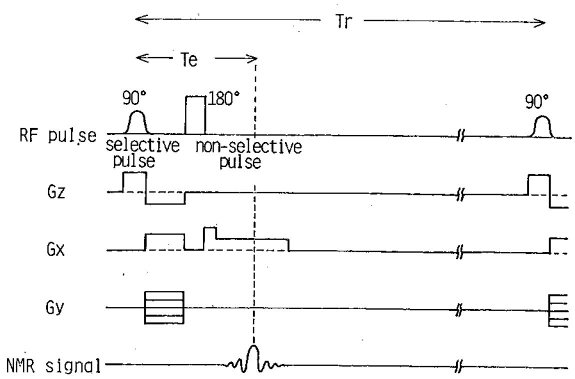

(b) Pulse sequence for saturation recovery method

Figure 1 Principles of magnetic resonance imaging.

2. Fast Recovery Method

2.1 Principle of nuclear magnetic resonance imaging method

Figure 1 shows the apparatus for the imaging method and a conventional pulse sequence named Saturation Recovery method (SR). Proton ^1H in uniform static magnetic field H_0 precesses in Larmor frequency ($\omega_0 = \gamma H_0$, γ is magnetic rotation ratio) and generates macroscopic magnetization M along the direction H_0 in thermal equilibrium. A narrow spectrum radio frequency (RF) pulse (frequency ω_0, 90 ° pulse) is applied to selectively excite a thin slice, M is nutated to the xy plane of the xyz coordinates, and the frame rotates at the Larmor frequency. Before the RF 180 ° pulse is applied, a gradient magnetic field Gx linear along the x axis is applied. After the 180 ° RF pulse, the echo signal is generated and detected with a gradient Gy linear along the y axis. After interval time T_r , this pulse sequence is repeated. The Gy is changed each pulse sequence and the location of ^1H on the x axis is identified from the phase of the echo signal. Also, Gx identifies ^1H on the y axis from Larmor frequency. Then, a two-dimensional image of ^1H density can be achieved by Fourier transform of the echo signals. In the conventional method to create a bigger echo signal, time interval T_r of sequences must be $T_r > 3T_1$ to return M to thermal equilibrium, where T_1 is spin-lattice relaxation time. For this reason, the SR method requires a long scan time. For example, if T_1 of the human brain is 0.3 - 0.5 s, $T_r > 1.5$ s, and the number of sequences n is 256, then the total scan time is 384 s. A longer scan time is required if the pulse sequence is repeated and the echo signals averaged to improve S/N. In practice, T_r 0.5 s is adopted to achieve good image contrast and reduce the scan time, but results in a poor S/N.

2.2 Principle of the fast recovery method

The pulse sequence of the FR method and the behavior of M in the rotational coordinate frame are illustrated in Fig. 2 (horizontal axis is time). The subscripts of RF pulses, x and y, indicate RF phase. The specimen is placed in H_0 which defines the z axis. First, a linear gradient field Gz is applied and a 90_x ° narrow spectrum RF pulse signal is used to selectively excite a thin slice. The 90 ° means that the pulse nutates the spins through 90 ° (the angle depends on the intensity-pulsewidth of the pulse) and the x subscript means that the rotation is 90 ° from the z axis to the y axis about the x axis; the axis of rotation depends on the RF phase shift. After 90_x ° , the phase shift gradient field Gy and the read-out projecting gradient field Gx are applied and free induction decay (FID) signals are produced. After T_s /2 seconds, nonselective 180_y ° pulse and gradient field Gx to cause a refocusing and resultant spin echo signal are applied successively. After T_s, the spin echo peak, a selective 90_x ° exciting pulse is applied and - together with Gz, which is a time-inverted mirror image of the first Gz - rotates the refocused spins in the slice to along the negative z axis. Then, all spins of the specimen are along the z-axis, but inverted. Immediately after the 90_x ° pulse, a nonselective 180_{-x} ° is applied to rotate all spins to the negative x-axis and restore the spin system to equilibrium. The spins do not completely recover equilibrium due to a T_2 dephasing effect during T_s , so before repeating the pulse sequence, it is necessary to wait a decay interval T_d for M to recover equilibrium spontaneously by natural relaxation. This pulse sequence runs continuously and the two read signals, FID and spin echo, are averaged to reconstruct an image by the Fourier Transform method. From the behavior of M shown in Fig. 2, it is clear that the FR method can drive the M of all areas of the specimen to equilibrium quickly and precisely without penalty of S/N, so that a short waiting time $T_d > T_1$ is required. The pulse sequence used in the “Driven Equilibrium Fourier Transform (DEFT)” method in conventional nuclear magnetic resonance analysis to shorten the data acquisition time would be difficult or impossible to apply to two-dimensional imaging. Because the M of an edge of a slice cannot be restored completely to

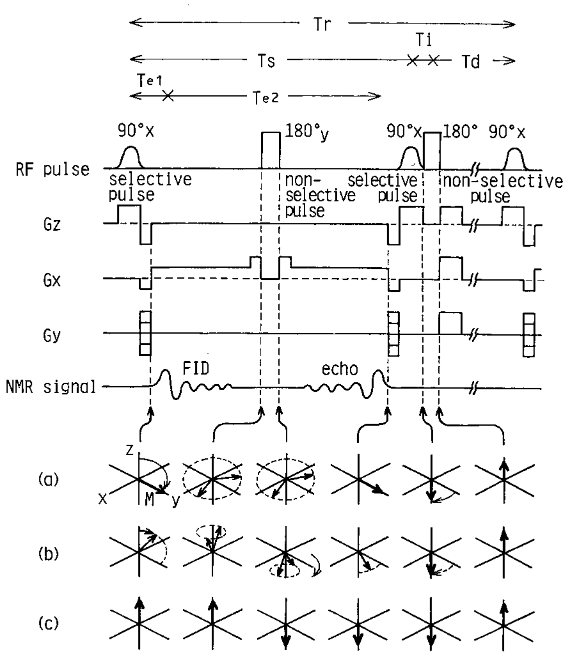

Figure 2 Pulse sequence for the fast recovery method.
Gz,Gx,Gy are gradient fields. Gz is parallel and Gx, Gy are orthogonal to magnetic field H_0.
(a), (b) and (c) illustrate the behavior of magnetization M. (a) In the center of the slice. (b) In the boundary area (on the surface of the slice). (c) Out side the slice.

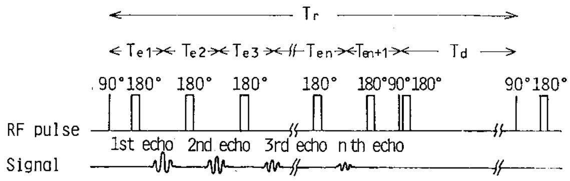

Figure 3 Using multiple echoes with the fast recovery method.

thermal equilibrium by DEFT, S/N is not improved and slice cross section is complex [9].

A variation of the FR method is shown Fig. 3. Other 180 ° pulses are applied between two 90 ° pulses and multi echo signals are generated. If the number of these 180 ° pulses is odd, 90 ° and 180 ° pulses are required to restore the M to equilibrium, and if even, only 90 ° pulses are required. It is possible to average these multi echo signals but S/N is not improved due to the T_2 effect during $T_{e1} + T_{e2} + T_{e3} + \cdots$.

3. Signal to Noise Ratio

In this section, the S/N is compared between the FRFID method which uses FIDs shown in Fig. 2 and the FRmSE method which uses multi spin echo (mSE); m is the number of echo signals shown in Fig. 3.

The maximum point of FID signal intensity in Fig. 2 is

$$S_{FID} = AM_0 \times \frac{1-2\exp\{-(T_r - T_s - T_I)/T_1\} + \exp\{-(T_r - T_s)/T_1\}}{1 - \exp\{-(T_r - T_s)/T_1 - T_s/T_2\}} \times \exp(-T_{e1}/T_2) \quad \cdots (1).$$

The signal intensity of the spin echo signal is

$$S_{SE} = S_{FID} \exp(-T_{e2}/T_2) \quad \cdots (2).$$

The image is reconstructed by averaging S_{FID} and S_{SE}, and noise, N, has no correlation. Thus, S/N is

$$(S/N)_{FID} = (S_{FID} + S_{SE}) / \sqrt{2}\, N \quad \cdots (3).$$

The maximum point of k 'th spin echo in Fig. 3 is

$$S_{kSE} = AM_0 \times \frac{1-\exp\{-(T_r - \tau)/T_1\}}{1 - \exp\{-(T_r - \tau)/T_1 - \tau/T_2\}} \times \exp(-\tau'/T_2) \quad \cdots (4)$$

where

$$\tau = \sum_{i=1}^{n+1} T_{ei}, \quad \tau' = \sum_{j=1}^{k} T_{ej}.$$

S/N by averaging all echo signals is

$$(S/N)_{mSE} = \frac{\sqrt{2}}{\sqrt{n}\, N} \cdot \sum_{k=1}^{n} S_{kSE} \quad \cdots (5).$$

In the following discussion, $T_{e1} = T_{e2} = \cdots = T_{en+1} = T_e$ is defined. Theoretical and experimental results using phantoms of signal intensity and T_r in FRFID, FR1SE and SR methods are shown in Fig. 4. Here, S/N of the SR method is

$$(S/N)_{SR} = \frac{AM_0}{N} \times \{1-2\exp\{-(T_r - T_e/2)/T_1\} + \exp(-T_r/T_1)\} \times \exp(-T_e/T_2) \quad \cdots (6).$$

These results show that the pulse sequences are precisely controlled. Also, the signal intensities are FRFID > FR1SE > SR and the shorter the T_r the bigger the difference among these.

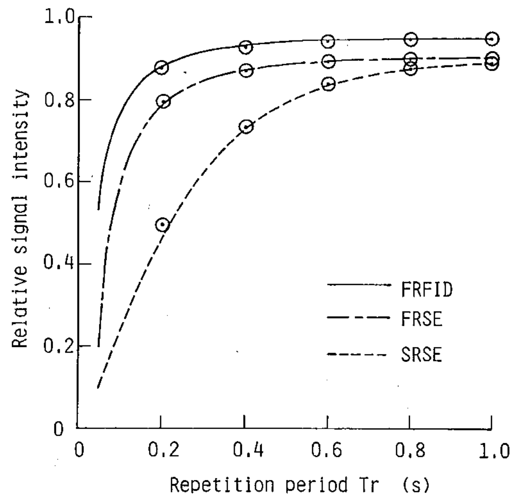

Figure 4 Relationship between relative signal amplitude and repetition period Tr, for FRFID, FR1SE and SR methods. The lines and circles respectively show calculated and experimental results using phantoms.

S/N of FRFID, equation (3), and FRnSE, equation (5), are compared in Fig. 5 where relative S/N is normalized by the S/N of FR1SE. T_1 and T_2 values of the human brain gray matter (GM) and cerebrospinal fluid (CSF) [12] are adopted. In Fig. 5(a), the larger m the lower S/N because the shorter T_d of a larger m sequence more effectively decreases the echo signal than by the echo signal averaging effect. In Fig. 5(b), the larger m gives a better S/N in the case of T_r > 500 ms, because echo signal averaging is more effective when T_2 > 600 ms of CSF. According to these results, the S/N of FRFID is 1.5 times better at T_r = 200 ms, and 1.9 times better at T_r = 100 ms than FR1SE. FRmSE with short T_r for fast scan shows a small improvement in S/N.

4. Scan Time

The scan time T_{FR}, T_{SE} and T_{SR} of the FRFID, FR1SE and SR methods respectively are discussed here. The scan time is expressed by

$$T = pnT_r \qquad \cdots (7)$$

where p is the number of averaging data and n is the number of pixels in a line. In the condition of constant n and same S/N, the scan time parameters are:

1) S/N is improved by p number at constant T_r.
2) T_r is selected to achieve the same S/N at constant p.

In the case of 1), the authors reported that the S/N of FRFID was 2 - 5 times larger than the SR method and $T_{SR}/T_{FR} = 2^2 - 5^2$ [9]. The practical SR method adopts T_r = 0.2 - 1 s, so case 2) is discussed here.

Figure 6 shows T_{SR}/T_{FR} and T_{SR}/T_{SE} for given S/N. The slice profile is a Gaussian function. T_{FR} is 1/4 of T_{SE} in T_r = 0.07 - 0.25 s of FRFID, and T_{SE} is 1/2 of T_{SR} in T_r = 0.1 - 0.5 s of FR1SE.

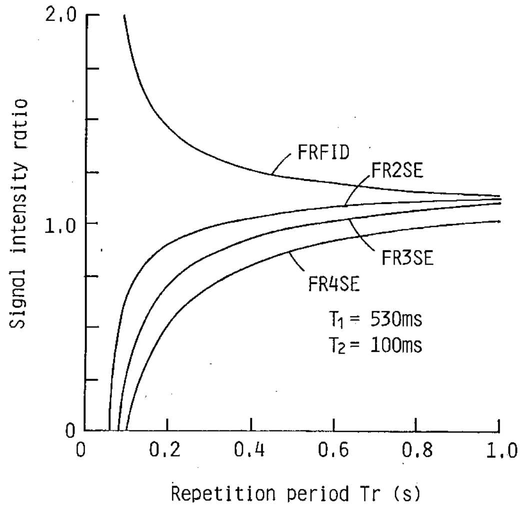

(a) for gray matter in human head

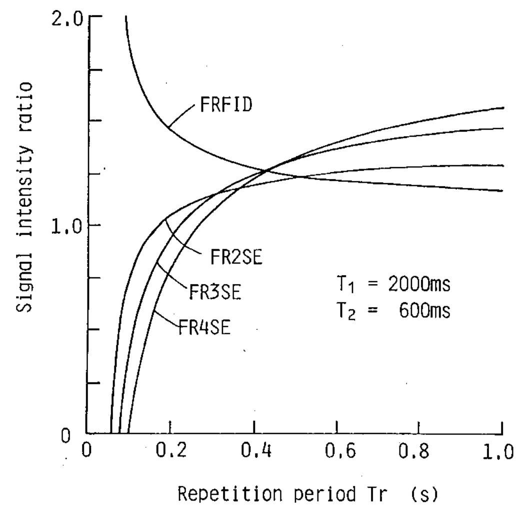

(b) for CSF in human head

Figure 5 Relative SN ratio for FRFID and FRmSE methods compared with FR1SE method as a function of repetition period Tr.

5. Relationship between S/N and Static Magnetic Field

S/N is proportional to H_0 when $T_r >> T_1$, and the results of improved S/N and short scan time using a high static magnetic field have been reported [4]. The relationship between S/N and the static magnetic field in FRFID is discussed here. T_1 of the human body depends on H_0 and is expressed by [14]

$$T_1 = C\nu^D \qquad \cdots (8)$$

Here, resonant frequency ν is $(\gamma/2\pi)H_0$, and C and D are constants depending on human tissues. For the human brain, $C = 1.52\times10^{-3}$ and $D = 3.48\times10^{-1}$ of white matter

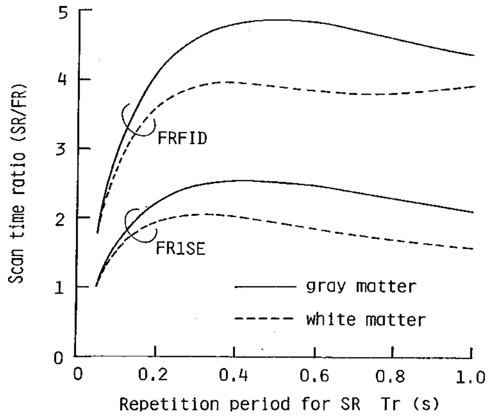

Figure 6 For given SN ratio, this graph shows ratio of scan time for FRFID and FR1SE methods to that for SR method, as a function of repetition period T_r.

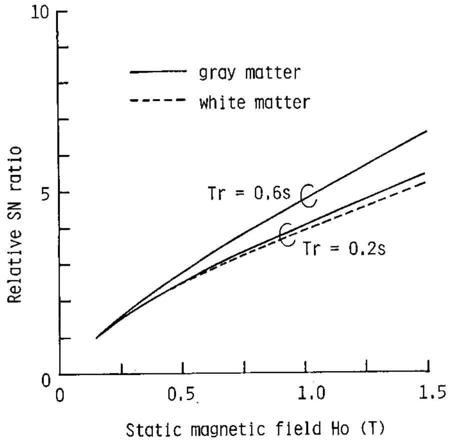

Figure 7 Relative SN ratio for SR method as a function of static magnetic field H_0 (for measurement on human head)

(WM), and $C = 3.62\times10^{-3}$ and $D = 3.08\times10^{-1}$ of gray matter (GM). S/N of the SR method (6) is expressed as follows including the H_0 effect of (8),

$$(S/N)_{SR} = \frac{AM_0}{N}$$

$$\times\{1-\exp\{-(T_r-T_e/2)/C\nu^D\}+\exp(-T_r/C\nu^D)\}$$

$$\times\ \exp(-T_e/T_2) \qquad \cdots\ (9).$$

Figure 7 shows the relationship between H_0 and relative S/N normalized by $(S/N)_{SR} = 1$ at $H_0 = 0.15T$. $(S/N)_{FID}$ at 0.15T is almost equal to that of $(S/N)_{SR}$ at 0.5T, because $(S/N)_{FID} / (S/N)_{SR}$ 3 [9].

6. Contrast Noise Ratio (CNR) among Tissues

Medical imaging diagnosis uses the image contrast to discriminate between normal tissues and pathological changes in physiological function and anatomical shapes. CNR due to changes in T_1 and T_2 by pathological changes was already reported [9]. CNR of anatomical shapes of the human brain tissues is analyzed below. Under the conditions that the scan time, image area, pixel size and data sampling time T_e are fixed, and the signals are averaged (T/T_r) times, the frequency bandwidth is

$$\Delta f = n\,(1/T_e) \qquad \cdots\ (10).$$

Noise is

$$N \propto \sqrt{T_r/T}\cdot\sqrt{1/T_s} \propto \sqrt{T_r/T_e} \qquad \cdots\ (11).$$

CNR is

$$CNR = \Delta S/N \propto \Delta S\sqrt{T_e/T_r} \qquad \cdots\ (12)$$

where ΔS is the signal difference between two tissues.

Figure 8 shows the CNR of GM, WM and CSF in SR and FR1SE methods with the parameters of $T_r = 1$ s, $T_e = 0.02$ s, $M_0 = 1$ of GM, A = 1, and CNR = 1 in $\Delta S = 1$. Maximum CNR between GM and WM is –0.12 by the SR method in $T_r = 0.2$ s and $T_e = 0.02$ s. But CNR is about zero in $T_r = 0.9$s where S/N is best. In FR1SE, CNR is about zero in T_r =

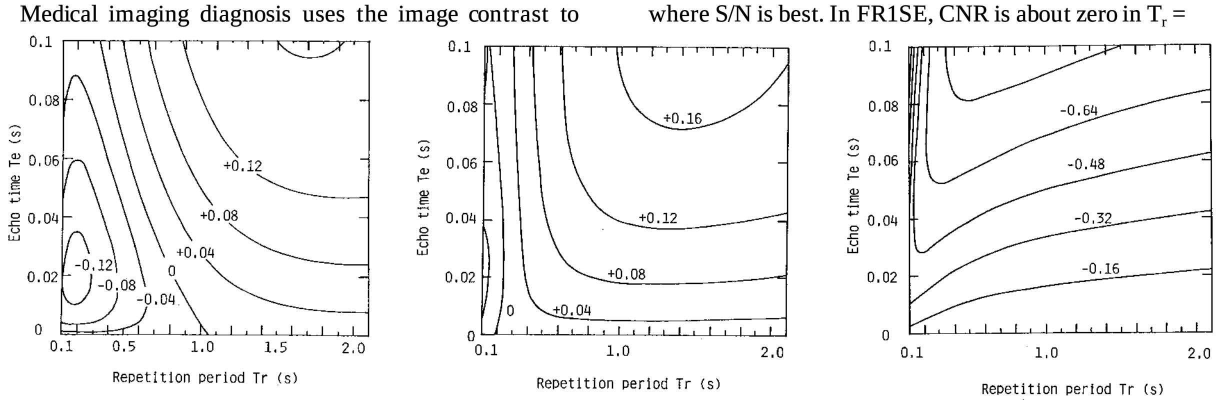

(a) CNR between GM and WM for SR method (b) CNR between GM and WM for FRFID method (c) CNR between GM and CSF for FRFID method

Figure 8 Relative contrast noise ratio(CNR) as a function of repetition period, T_r, (relative to CNR for T_r =1s, T_s = 0.02s, M_0(GM) =1, A =1 and S =1)

0.2s and 0.08 in $T_r > 0.5$ s where S/N is better. Also, CNR between GM and CSF is good, –0.32, in $T_r = 0.1 - 0.2$ s. CNR of FRFID is almost the same as that of FR1SE. These results showed that CNR of the FR method between normal human brain tissues is low for a shorter scan time, $T_r = 0.1 - 0.2$ s, and has good contrast with high S /N in $T_r > 0.5$ s.

7. Experimental results

Measurements were made using a four-coil resistive magnet with 0.15T field in a whole body MRI machine designed by the authors, show n in Photo. 1. The magnetic field uniformity including time drift is ±20 ppm. Photo. 2 shows the images of the SR and FR1SE methods for the same S/N and that $T_{SR}/T_{FR} = 3$, the same as Fig. 6. The images of FRFID are shown in Photo. 3; (a) is a fast-scan image with $T_r = 0.1$ s and $T_{FR} = 25.4$ s but low contrast between WM and GM, and (b) is a high contrast and S/N image of ^{1}H density with $T_{r=}$ 1 s and $T_{FR} = 254$ s.

8. Conclusions

This paper gave a theoretical analysis and experimental results of the human body of FRFID and FRmSE, in terms of S/N, scan time and CNR of images. The results can be summarized as follows.

1) The first images of a human head using the FR method were obtained.
2) S/N of FRFID and FRmSE was analyzed as: FRFID > FR1SE > FRmSE (m ≧ 2).
3) The scan time of FRFID was 1/4 of SR and that of FR1SE was 1/2 for the same S/N images, with $T_r = 0.07 - 0.25$ s of FRFID and $T_r = 0.1 - 0.5$ s of FR1SE.
4) FRFID was better than FRmSE in S/N and scan time, whereas FRmSE was better for non-uniformity of static magnetic field due to the use of 180° pulses and echo signals.
5) S/N of the FR method using a 0.15T magnet was the same as that of the SR method using a 0.5T magnet. This indicates that the FR method reduces the system cost.
6) CNR of the FR method was analyzed and demonstrated in human images. The fast-scan images of $T_r = 0.1 - 0.2$ s showed low CNR and the images of $T_r > 0.5$ s showed high CNR and S/N.

The FR method is a new algorithm to control macroscopic magnetization and shorten the scan time using new RF pulse sequences. FR has advantages such as no additional cost is required because a stronger magnetic field is not needed, and by changing the pulse sequence program a conventional MRI machine can be changed to a fast-scan machine. In order to control the macroscopic magnetization M precisely, a stable RF pulse and gradient field of the machine are required. In future work, we will optimize the parameters of the FR method for diseases by clinical testing on patients.

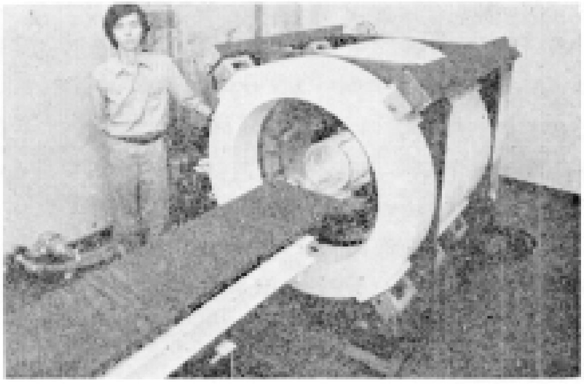

Photograph 1 photograph of the resistive magnet

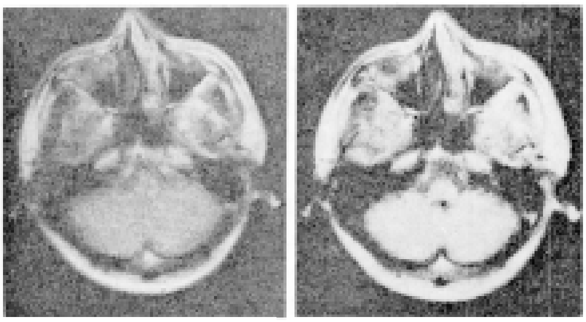

(a) An SR image for T_r =0.72s, n=511, and T=368s

(b) An FR1SE image for T_r =0.24s, n=511, and T=123s

Photograph 2 Images of human head

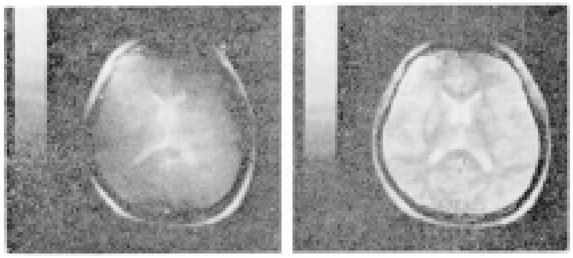

(a) Fast-scan image for FRFID method, T_r =0.1s, p=2, n=127, and T=25.4s

(b) High quality Image for FR1SE, T_r =1s, p=2, n=127, and T=254s

Photograph 3 Images of human head

Acknowledgment

The authors wish to express their gratitude to Dr. Akira Ohte for his support and encouragement.

References

[1] P.C. Lauterbur: Image Formation by Induced Local Interactions: Examples Employing Nuclear Magnetic Resonance, Nature, 242, 190/191 (1972)

[2] J.M. McNally and G.C. Hurst: Driven Equilibrium Fourier Transform Imaging of Proton/Phosphorus Nuclei in 2.0T Whole Body Magnet, Proc. Soc. Magn. Reson. Med., 1028/1029 (1985)

[3] Haase, et al: Rapid Images and NMR Movies, Proc. Soc. Magn. Reson. Med., 980/981 (1985)

[4] W.A. Edelstein, et al: NMR images of the Human Trunk at 64MHz, Proc. Soc. Magn. Reson. Med., 116/117 (1983)

[5] P. Mansfield, et al: Dynamic Imaging by NMR, Proc. 3rd World Congress of Nuclear Medicine and Biology, 3575/3576 (1982)

[6] D. Ratzel, et al: Fast NMR Head Tomograms, Proc. Soc. Magn. Reson. Med., 128/129 (1982)

[7] L. Crooks, et al: Nuclear Magnetic Resonance Whole-Body Imager Operating at 3.5k Gauss, Radiology, 143-1, 169/174 (1982)

[8] W.S. Hinshaw: Image formation by Nuclear Magnetic Resonance: The Sensitive-point method, J. Appl. Phys., 47-8, 3709/3721 (1976)

[9] H. Iwaoka, T. Sugiyama, H. Matsuura and K. Fujino: A New Pulse Sequence for “Fast Recovery” Fast-Scan NMR Imaging, IEEE Trans. Medical Imaging, MI-3-1, 41/46 (1984)

[10] H. Iwaoka, T. Sugiyama and H. Matsuura: Fast Scan NMR Imaging Method (2), Proc. 4th Nuclear Magnetic Resonance in Medicine (Japanese), 222/223 (1984)

[11] H. Iwaoka, T. Sugiyama and H. Matsuura: Fast Scan NMR Imaging System, Proc. 23rd Society for Instrumentation and Control Engineers Annual Meeting (Japanese), 333/334 (1984)

[12] T. Hirata, H. Matsuura, T. Sugiyama and H. Iwaoka: T_1, T_2 and Proton Density Computed Images in NMR-CTMR Imaging System, Proc. 6th Nuclear Magnetic Resonance in Medicine (Japanese), 115 (1985)

[13] D.I. Hoult and P.C. Lauterbur: The Sensitivity of the Zeugmatographic Experiment Involving Human Samples, J. Magn. Reson., 34, 425/433 (1979)

[14] P.A. Bottomley, et al.: A Review of Normal 1H NMR Relaxation Times from 1 - 100MHz: Dependence on Tissue Type, NMR Frequency, Temperature, Species, Excision, and Age, Proc. Soc. Magn. Reson. Med., 70/71 (1984)

Hideto Iwaoka (Member)

He received the B.E., M.E., and Dr.Eng. degrees in electrical engineering in 1969 ,1971 and 1987, respectively, from Keio University, Japan.

In 1971 he joined Yokogawa Electric Corporation, Tokyo Japan, and engaged in the development of Nuclear Quadrupole Resonance thermometry, Magnetic Resonance Imaging, Optoelectronic devices, Microwave devices, and Micromachining devices. He is now a General Manager of Strategic Technology Planning Department of Yokogawa Electric Corporation.

Dr. Iwaoka was awarded the Best Paper Awards in 1988 and 1999 from the Society of Instrument and Control Engineers in Japan, and the Patent Awards in 1978 and 1999. He is a member of the Society of Instrument and Control Engineers in Japan, the Japan Society of Applied Physics, The Institute of Electrical Engineers of Japan, and IEEE.

Hiroyuki Matsuura (Member)

He received the B.S. and M.S. degrees in electronic engineering from the Tokyo Institute of Technology, Tokyo, Japan, in 1978 and 1980, respectively. In 1980, he joined the Yokogawa Electric Corporation, Tokyo, Japan, where he was engaged in the research of medical imaging apparatuses and the circuit design for high-speed/high-frequency measuring instruments. From 1990 to 1992, he was a Visiting Scholar at Stanford University, Stanford, CA. Mr. Matsuura was the recipient of the 1998 Society of Instrument and Control Engineers Best Paper Award. He is a member of the Society of Instrument and Control Engineers (SICE), the Institute of Electrical and Electronics Engineers (IEEE) and the Instrument of Electronics, Information and Communication Engineers (IEICE).

Tadashi Sugiyama (member)

He received the B.E. degree from Waseda University, Tokyo, Japan, in 1978 .Since joining Yokogawa Electric Corporation in 1978, he has been engaged in the development of Magnetic Resonance Imaging and optical measurement instruments. He received Awards from Society of Instrument and Control Engineers of Japan in 1988 and 1989. Mr. Sugiyama is a member of the Society of Instrument and Control Engineers of Japan and the Japan Society of Applied Physics.

Takaaki Hirata (Member)

He received the B.E. degree in pure and applied sciences in 1981, and the M.E. and Dr.Eng. degrees in applied physics in 1983 and 1992, respectively, from the University of Tokyo, Tokyo, Japan.

In 1983 he joined Yokogawa Electric Corporation, Tokyo Japan, where he was engaged in the development of Magnetic Resonance Imaging, Optoelectronic Devices and Photonic Integrated Circuits. He is now a Manager of Optoelectronics Laboratory of Yokogawa Electric Corporation.

Dr. Hirata is a member of the Society of Instrument and Control Engineers in Japan and the Japan Society of Applied Physics. He received the SICE Paper Award in 1988, the SICE Technology Awards in 1994 and 2001, and the MOC Paper Award in 1995.

Reprinted from Trans. Of the SICE, Vol.23, No.4, 326/332 (1987)